Photonic crystal and photonic wire device structures

Richard De La Rue, Marc Sorel, Nigel Johnson, Faiz Rahman, Charles Ironside, et al.

Richard De La Rue, Marc Sorel, Nigel Johnson, Faiz Rahman, Charles Ironside, Lee Cronin, Ian Watson, Robert Martin, Chongjun Jin, Pierre Pottier, Harold Chong, Marco Gnan, Aju Jugessur, Edilson Camargo, Grant Erwin, Ahmad Md Zain, Iraklis Ntakis, Lois Hobbs, Hua Zhang, Mario Armenise, Caterina Ciminelli, Dominique Coquillat, "Photonic crystal and photonic wire device structures," Proc. SPIE 5950, Photonic Crystals and Fibers, 595004 (12 October 2005); doi: 10.1117/12.620658

Event: Congress on Optics and Optoelectronics, 2005, Warsaw, Poland

Photonic Crystal and Photonic Wire Device Structures

Richard De La Rue, Marc Sorel, Nigel Johnson, Faiz Rahman, Charles Ironside, Lee Cronin [a], Ian Watson [b], Robert Martin[c], Chongjun Jin, Pierre Pottier, Harold Chong, Marco Gnan, Aju Jugessur [d], Edilson Camargo [e], Grant Erwin, Ahmad Md Zain, Iraklis Ntakis, Lois Hobbs, Hua Zhang, Mario Armenise[f], Caterina Ciminelli[f], Dominique Coquillat[g]
University of Glasgow, U.K., e-mail: r.delarue@elec.gla.ac.uk
[a] Chemistry Department, University of Glasgow, U.K.
[b] Institute of Photonics, Strathclyde University, U.K.
[c] Physics Department, Strathclyde University, U.K.
[d] McGill University, Montreal H3A 2A7, Canada
[e] Centro Técnico Aeroespacial, Brasil,
[f]Politecnico di Bari, Italia
[g]GES,Université Montpellier-2, France

Summary

Photonic devices that exploit photonic crystal (PhC) principles in a planar environment continue to provide a fertile field of research. 2D PhC based channel waveguides can provide both strong confinement and controlled dispersion behaviour. In conjunction with, for instance, various electro-optic, thermo-optic and other effects, a range of device functionality is accessible in very compact PhC channel–guide devices that offer the potential for high-density integration. Low enough propagation losses are now being obtained with photonic crystal channel-guide structures that their use in real applications has become plausible. Photonic wires (PhWs) can also provide strong confinement and low propagation losses. Bragg-gratings imposed on photonic wires can provide dispersion and frequency selection in device structures that are intrinsically simpler than 2D PhC channel guides - and can compete with them under realistic conditions.

1. Introduction:

This paper is mostly concerned with the results of recent research activity carried out by the above authors. This work includes studies of techniques for growing close to perfect multi-layer, 3D-periodic, opal photonic crystals (PhCs) with fcc or near fcc structure - and the (100) lattice orientation that can be obtained from a template-consisting of a square array of pillars with an appropriate spacing in relation to the diameter of the colloidal spheres that form the opal crystal. The controlling influence of the templates used is sufficiently strong that significant distortion towards a tetragonal structure has been sustained at the same crystal quality. An example of such a structure is shown in Fig. 1 [1]. Crystals with the same level of regularity and perfection throughout areas as large as 1 mm^2 have been produced by this technique – but this area was solely determined by the size at which a suitable high resolution electon-beam lithography (EBL) field could be written. So the growth technique is inherently capable of producing the same level of perfection over considerably larger areas. The quality of the photonic

Photonic Crystals and Fibers, edited by Waclaw Urbanczyk, Bozena Jaskorzynska, Philip S. J. Russell,
Proc. of SPIE Vol. 5950, 595004, (2005) · 0277-786X/05/$15 · doi: 10.1117/12.620658

crystal produced by this template-controlled capillary growth technique is directly related to the size dispersion of the colloidal spheres from which it is produced – indicating that further work on controlling the sphere formation process would be worthwhile.

Another area of activity that will be mentioned only in this introduction is the production of regular arrays of pyramidally shaped structures based on large-bandgap group III nitride semiconductors [2]. The structures shown were realised using the selective area growth (SAG) technique, in conjunction with electron-beam patterned arrays of holes in the silica mask layer used for the SAG process. Earlier work showed that structures produced with a substantially larger lattice period were very regular – and had a measurable photonic crystal behaviour, although this behaviour was observed only at much longer wavelengths than the blue part of the visible spectrum. These pyramidal SAG structures also had quantum wells grown into them, making both cathodo-luminescence and photo-luminescence available in the blue part of the spectrum.

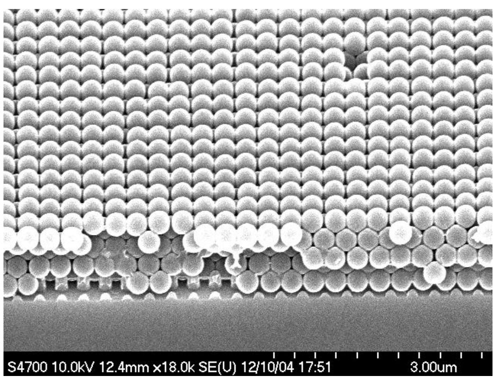

Fig. 1: Regular opal structure grown with (100) orientation on template substrate.

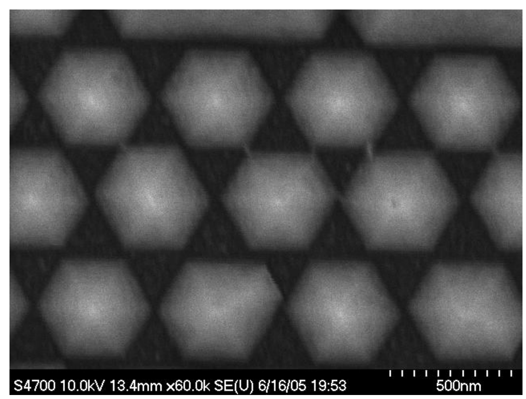

Fig. 2: Hexagonal-base shape GaN-based SAG pyramidal structures.

In the following text, research on *photonic-crystal* (PhC) and *photonic-wire* (PhW) structures in the high refractive index semiconductor systems, silicon-on-insulator (SoI) and gallium arsenide/aluminium gallium arsenide (GaAs/AlGaAs) will be reviewed. Results obtained on thermo-optically operated PhC Mach-Zehnder modulators and thermo-optically tuned PhC cavity resonators will be described, including device structures in which short 2D PhC sections act as mirrors or separators in relatively wide (i.e. 'normal' width or even multi-mode) ridge waveguides. These devices include coupled-cavity filter structures, extended Fabry-Perot cavities and T-junction beam-splitters. Finally we shall describe computational analysis of the behaviour of photonic-wire type Bragg grating structures over a wide range of operating spectrum, showing that low-loss and high-reflectivity can be obtained under suitably chosen operating conditions, but also that such structures can also act as directional antennas that couple effectively to lateral radiation.

Before entering into consideration of specific PhC and PhW devices, we remind the reader of some of the reasons why several common semi-conducting materials are important in this field. High purity silicon is widely available in the form of large-area wafers, currently mostly at a diameter of eight inches (20 cm.), with twelve inches (30 cm.) well in view. For the present purposes, the form in which there is a thin layer of silicon firmly bonded on top of a buffer layer of silica is the important one. High quality 6 inch (12 cm) diameter gallium arsenide wafers are also readily available – and somewhat smaller diameter indium phosphide (InP) wafers likewise. Silicon, germanium and the III-V semiconductors such as gallium arsenide and indium phosphide have characteristically high refractive indices – above three for all the materials specifically named in this sentence. All of the examples specifically cited exhibit electronic band-gaps/absorption-edges in the near infra-red, implying transparency at longer wavelengths - and photo-detection capability at shorter wavelengths. Direct-bandgap III-V semiconductors in binary, ternary, quaternary and even pentary composition formats can provide current-injection electroluminescence with un-surpassed electrical-to-optical (electron-photon) conversion efficiencies.

2. PhC channel-waveguide devices

One of the basic devices of planar waveguide-based integrated optics/photonics is the Mach-Zehnder (MZ) structure, which can be used conveniently as both modulator and switch. We have specifically realized thermo-optically operated photonic crystal channel waveguide Mach-Zehnder modulators, as shown in Fig. 3 and Fig. 4, in both symmetric [3, 4] and asymmetric [5] forms. For the former configuration, the transmitted light is close to a maximum value in the absence of heat applied locally through a NiCr thin-film electrode pattern covering part of one arm of the structure – and is then reduced to a minimum with a 14 dB on-off ratio when approximately 40 mW is applied through the electrode. These results were obtained for a structure fabricated in AlGaAs/GaAs epitaxial waveguide material that provided only weak confinement. With a somewhat improved heater electrode design, an asymmetric M-Z structure fabricated in silicon-on-insulator waveguide required only 25 mW of heater power to go from the transmission minimum at zero heater current to a transmission maximum. The asymmetry implemented used one branch having *two* extra holes in the length of the two diagonal parts of one arm of the structure. With the intrinsic 60^o-30^o -90^o geometry of the structure, this increase in the diagonal lengths implies a reduction by *two* holes in the length of the parallel guide part of the arm – and a total net relative length difference of two hole spacings, between the two arms.

Further improvement is to be expected in the performance, e.g. in the extinction ratio, of PhC channel guide Mach-Zehnder structures - through improvements in the quality of the fabrication processes used. Electrical power requirements for thermooptic operation should also be significantly reducible by using various improvements in the design of the structure, i.e direct delivery of ohmic heating in the waveguide core and reduction of the possibilities for heat spreading away from the core region. It is interesting to note that quite similar performance has been obtained in Mach-Zehnder modulators while using very different planar waveguide material, i.e. SoI waveguide material in some cases and AlGaAs/GaAs waveguide material in others.

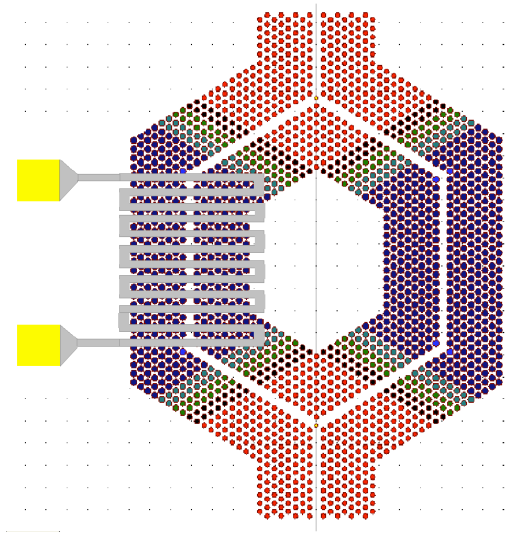

Fig. 3: Schematic of specification for EBL generated pattern of thermo-optic PhC channel-guide M-Z modulator.

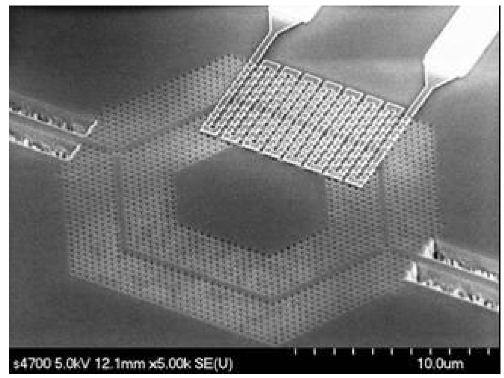

Fig. 4: Scanning electron micrograph of the M-Z modulator, showing superimposed NiCr thin-film heater electrode.

3. Photonic Wire Mach-Zehnder

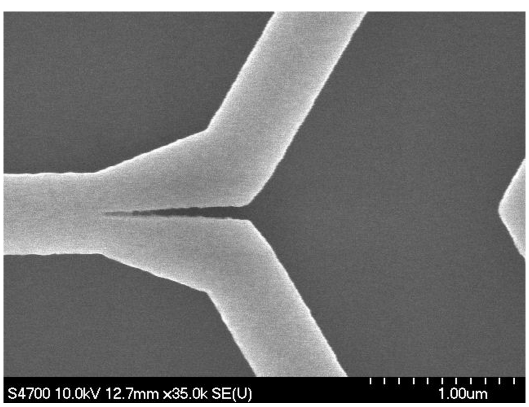

Fig.5: Detailed view of Y-junction section of PhW M-Z structure.

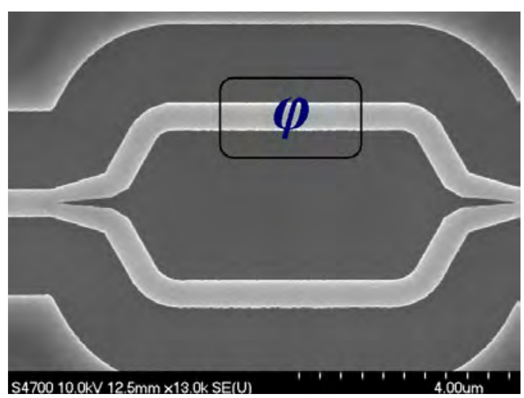

Fig. 6: Scanning electron micrograph of asymmetric PhW Mach-Zehnder structure, with schematic phase-shift.

More recently we have realized very compact M-Z structures in photonic wire waveguides, using the same SoI material as for our PhC work based on SoI. A substantial effort was dedicated to optimising the junctions and bend sections using a basic waveguide design that has a 260 nm thick silicon core layer and wire width of 500 nm. At this width, the PhW guide is almost single-mode for TE polarization. The optimization was performed manually using an FDTD simulation tool. Although useful experimental results have been obtained on the structures actually fabricated, we shall not report on them here.

4. PhC mirror coupled micro-cavity filter

We have investigated several device possibilities based on the embedding of photonic crystal structures in relatively wide and deep ridge waveguides. In such devices, 2D photonic crystal structures of quite limited extent along the main propagation axis, i.e. no more than five rows, can provide controlled reflectivity or useful beam-splitting capabilities. One example is a coupled cavity structure designed to provide a wider transmission band and steeper skirts in the frequency domain [6]. The configuration that we have investigated was realised with deeply etched holes in AlGaAs/GaAs epitaxial heterostructure waveguides. The three rows of holes forming the middle PhC region acted as a partial mirror and coupling section for the two cavities formed by the short spacer sections and the two exterior mirrors that were also formed by three rows of holes. The significant difference between the measured spectral response of the structure and the results of 2D simulation were attributable primarily to a quite modest difference between the specified hole diameter and that actually fabricated.

5. PhC Mirror Fabry-Perot filters

Another example of a waveguide-embedded cavity filter structure using PhC mirrors is shown in Fig. 7. This extended, but still compact (8 μm length), Fabry-Perot cavity [7, 8] is designed to have multiple resonances within the wide frequency stop-band defined by the mirrors. A measure spectral response is shown in Fig. 8. The design gives a specific resonance in the desired telecommunications operational wavelength range, with sufficient frequency tunability being possible via angular tuning or (potentially) by thermo-optic tuning. The experimentally achieved Q-factor of about 2000 is already large enough for dense wavelength-division multiplexing (DWDM) applications such as wavelength channel add-drop functionality. A combination of improvements in fabrication technology, 3D-simulation and careful re-design can reasonably be expected to give Q-factor values appropriate for application at the finest DWDM channel-spacing likely to be implemented in the near-future, without recourse to a strictly membrane waveguide format.

The original concept for this filter was to use angular tuning, taking advantage of the fact that the PhC mirror reflectivity does not change significantly over a usefully wide range of angles. But, for thermo-optic operation, we have also constructed a version of this device in SoI waveguide with a NiCr thin-film heater electrode, on top of a 300 nm thick CVD silica upper-cladding/buffer layer. The un-expected result of this approach, distinctly different from the results for the previously investigated thermo-optically tuned

PhC cavity in the same material system, was that heating the electrode led to a small *blue*-shift in the resonance spectrum, as illustrated in Fig. 9. (Applying approximately 2 mW gave a shortening of the wavelength by ~0.06 nm.) The expectation was, as in our previous thermo-optically controlled cavity device, that a relatively large index change in the silicon waveguide core would predominate, leading to rapid *red*-shifting when the device temperature was increased. The fact that much slower blue-shifting was obtained is attributable to a combination of several factors – of which the most significant is probably that the heat flow into the silicon waveguide core was sufficiently impeded by the silica buffer layer that the core temperature rise was much smaller than that of parts of the silica cladding.

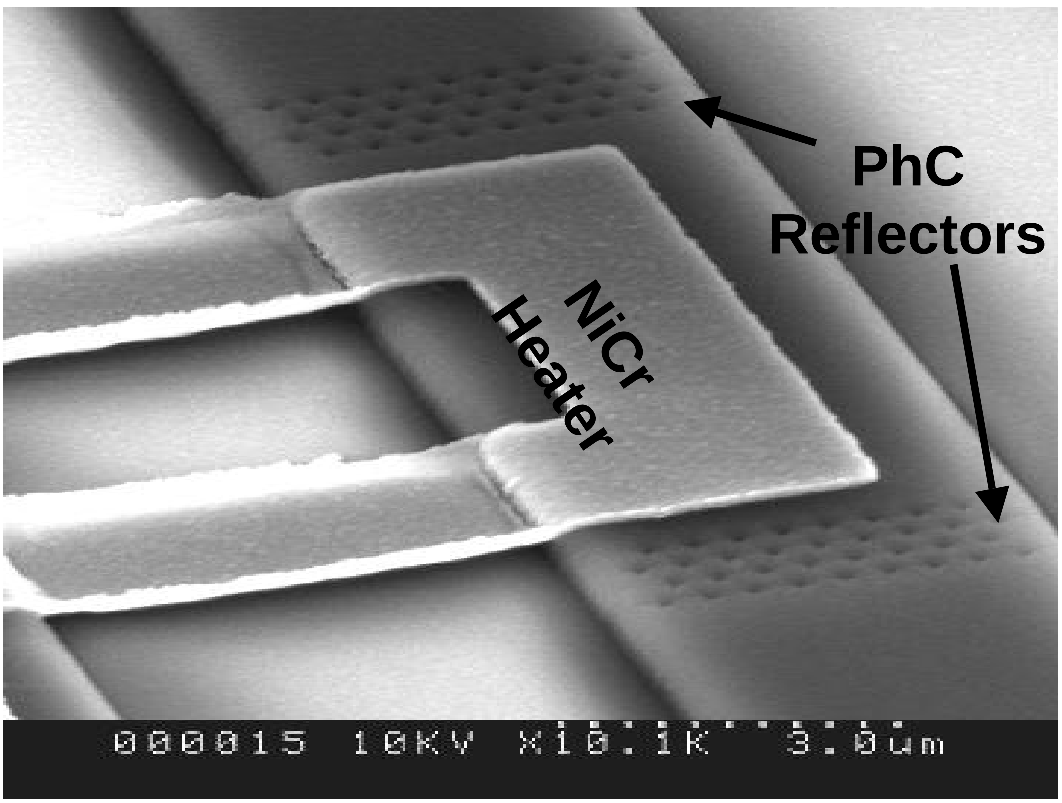

Fig. 7: Scanning electron micrograph of the PhC mirror extended Fabry-Perot micro-cavity realised in a section of SoI wafer, showing the NiCr heater film and gold feeder electrodes. The etched silicon core of the structure has been covered uniformly with 300 nm of silica deposited by plasma-enhanced chemical vapour deposition (PECVD), prior to deposition of the metallisation and formation of the electrodes.

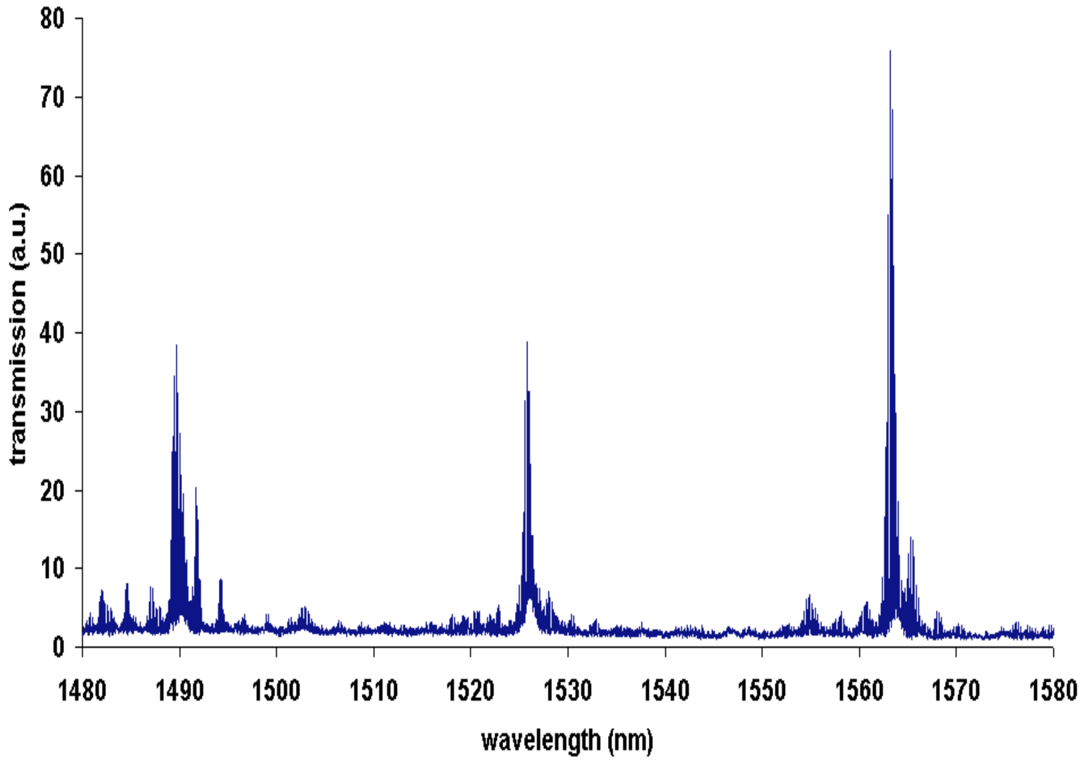

Fig. 8: Spectral response of PhC mirror F-P filter.

The thermal situation in the device is sufficiently complex that we have not attempted a full analysis, which would require a combination of a detailed analysis of the heat flow, together with modelling of stress/strain optical effects – and the optical modal distribution. In this context, it should be noted that the localised application of heat automatically induces stress and strain through differential thermal expansion between the constituent materials of the waveguide system – and that a process such as thermal oxidation of silicon to grow a silica cladding layer induces stress and strain for the same reason. It should be further remembered that silica alone has a net thermally-induced optical-path length change that is much smaller than that for silicon and of opposite sign – because thermal expansion has a larger (and opposite) effect on path length than refractive index change. An interesting example of the use of strain-optical effects in a silica-silicon 'photonic crystal' (in this case a 1D periodic mirror stack) to obtain a largely *athermal* (temperature independent) situation is given in [9]. But we can now go a step further and identify the possibility of realising very compact photonic crystal devices, such as WDM filters, that are intrinsically temperature-independent at the chosen wavelength because of the overall balance of effects, including the optical modal distribution – but such devices can additionally be tuned thermo-optically by selecive heating in chosen locations. In particular, delivering the required heating effect by passing electric current through the silicon core to obtain direct ohmic heating that originates in the core alone [10, 11] could achieve the required behaviour.

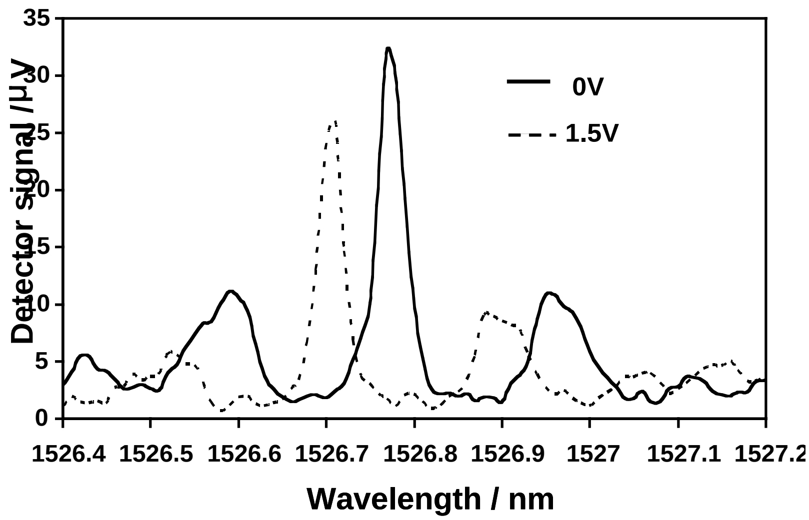

Fig. 9: Demonstration of blue-shift of the filter response when the heater electrode is switched on at 1.5 V. Notice the small level of the *blue*-shift produced, only ~ 0.06 nm. Individual spectral features observed are produced by double F-P cavity behaviour associated with sample ends.

6. PhC mirrorT-junction beam-splitter

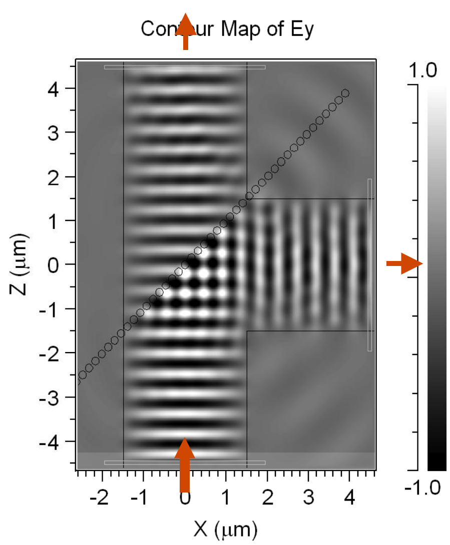

Fig. 10: Simulation of PhC T-junction beam-splitter.

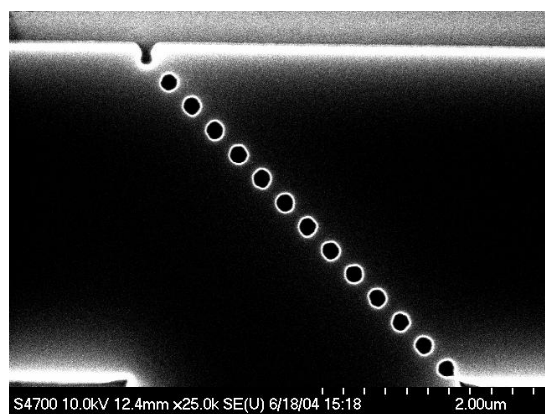

Fig. 11: Micrograph of PhC T-junction beam-splitter.

As a final example of a compact photonic crystal structure embedded in an optical waveguide of significant width (i.e. one that may be strictly multimode), we describe briefly work on a right angle T-junction beamsplitter, Fig. 10 and 11. The splitter uses either a single row of holes inclined at 45^o to the incoming and sideways reflected beams [12] or a three-row triangular (hexagonally-packed) lattice PhC, also inclined at 45^o. It emerges that such simple structures can provide interesting and potentially useful properties over usefully wide optical bandwidths, e.g the combination of close to equal power-splitting in one polarization (TM) and nearly complete transmission into the 'straight-ahead' branch. These properties can obtained with small values for the (~1%) losses that are caused by diffraction out of the structure.

We have carried out both 2D and 3D FDTD simulations using commercial software on such beam-splitting photonic crystal elements realised in several micrometer-wide waveguides realized in SoI, using an effective index approach in the 2D case to cover the effect of variation in the 'vertical' dimension. There is a significant shift along the frequency/wavelength axis between equivalent points for the 2D and 3D calculations – and the comparison between the results for the two alternative approaches is on-going. Experimental results have been obtained for both single-row and three-row PhC with nominal area filling-factors of 0.60 – and these results show a substantial level of agreement with the simulation results. This work is the subject of a full paper in preparation. Comparative results for selected situations appear in Fig. 12 and 13.

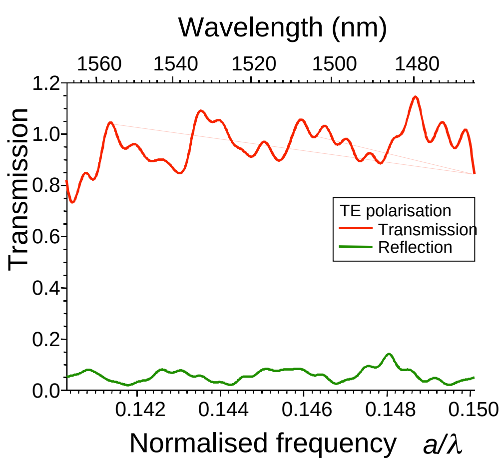

Fig. 12: Separation between Transmission and Reflection for TE polarisation only.

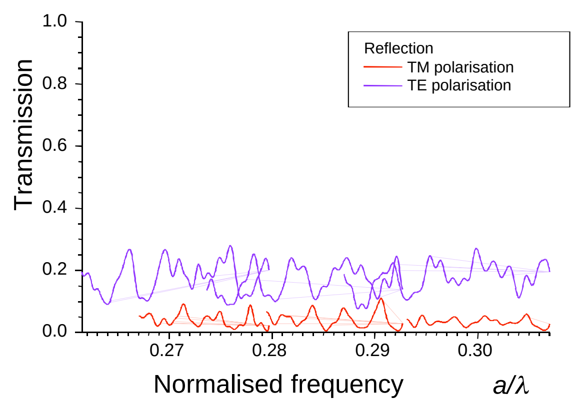

Fig. 13: Separation between TM and TE polarisation for Reflected light port.

7. Photonic wire Bragg gratings

Fig. 14 and 15 show, respectively, a scanning electron micrograph of a PhW first-order Bragg grating designed for operation at λ_o ~1550 nm, using SOI with a silicon core thickness of 260 nm - and its measure spectral response.

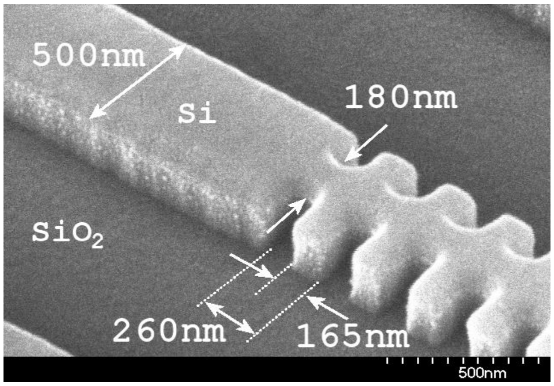

Fig. 14: PhW Bragg-grating in SoI waveguide.

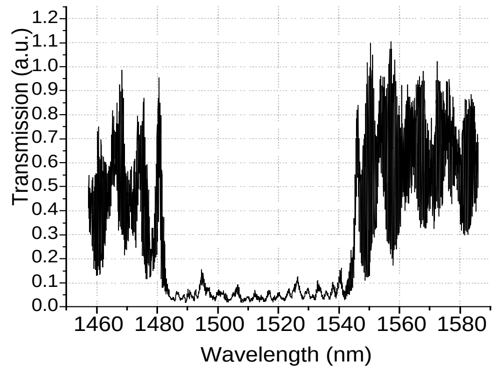

Fig. 15: Spectral response of PhW Bragg-grating.

Even for Bragg-grating structures realised in a photonic-wire waveguide geometry, with strong confinement and only 1D periodicity, it is clearly very desirable to use 3D computational modelling if accurate prediction of the behaviour of the structure is sought. A fully 3D approach also becomes more important if an attempt is to be made on modelling the impact of geometrical deviations of the structures actually fabricated from the ideal ones specified. But a substantial level of understanding of the behaviour of the SoI waveguide PhW Bragg-grating can be obtained by using an approach in which the computational task is simplified by treating two distinct 2D approximate representations of the device. One representation use a 2D in-plane description, together with an effective local refractive index description of the waveguide. This representation can readily show (approximately) the conditions under which the grating may become an antenna radiating light laterally out of the waveguide The second representation used allows for modelling of radiation out-of-plane. Particular situations for strong reflection with minimal loss – and for strongly radiative in-plane situations are shown schematically in Fig. 16 and 17.

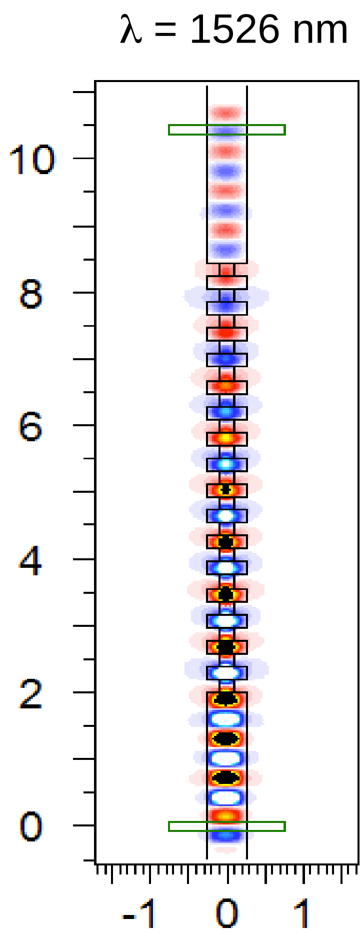

Fig. 16: Simulation of PhW Bragg-grating acting as strong reflector..

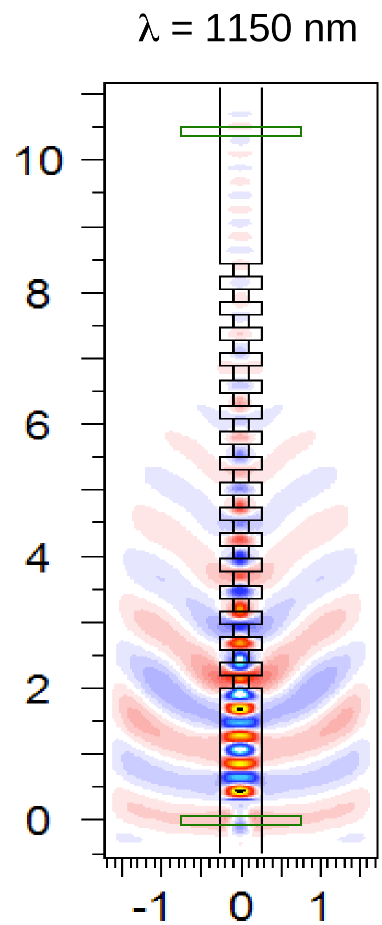

Fig. 17: Simulation of PhW Bragg-grating acting as radiative antenna.

8. Conclusions

It seems likely that photonic wire structures will compete successfully with photonic crystal channel waveguide structures in a variety of situations. The high index contrast and resulting strong confinement obtainable in the photonic wire waveguide format are favourable for enhancement of non-linear effects - and potentially also for low threshold lasers. Suitably-designed channel waveguides embedded in 2D photonic crystal structures can give even higher confinement than photonic wires - and become particularly interesting in situations where the periodicity along the channel contributes specific dispersion properties such as a transmission stop-band or slow-wave behaviour. Bragg-grating structures incorporated into a photonic wire geometry have already demonstrated that 1D-periodicity is sufficient for some applications. The extent to which the photonic wire Bragg-grating structure can provide specific dispersion characteristics, as well as sufficiently small propagation losses, requires further exploration

Thermo-optic effects can provide useful tuning and modulation behaviour in photonic crystal and photonic wire device structures, e.g. Mach-Zehnder modulators and in micro-cavities. Athermal operation of PhC devices based on 2D PhCs may possibly be attainable [9], particularly in the SoI system, but will require careful design and accurate control of associated stress/strain properties. If properly designed, compact thermo-optic devices in either PhC or PhW form can be both fast (<~1 ns switching time) and exhibit low-power (sub-milliWatt) operation [10, 11]. Practical planar PhC device production will also require mass-fabrication techniques, e.g. deep UV lithography and/or nano-imprint lithography.

9. References

1. C.Jin et al, paper presented at CLEO-Europe, Munich, June 2005.
2. I.M. Watson et al, paper presented at British Association for Crystal Growth (BACG) Annual Meeting, Sheffield, 4th to 6th September 2005.
3.E.A Camargo, A.S. Jugessur, I. Ntakis and R.M. De La Rue, "Photonic crystal waveguide Mach-Zehnder structures for thermo-optic switching", in Integrated Optical Devices: Fabrication and Testing, edited by Giancarlo C. Righini, Proc. SPIE 4944, pp. 376-381, (2003).
4. E.A. Camargo, H.M.H. Chong and R.M. De La Rue, '2D Photonic crystal thermo-optic switch based on AlGaAs/GaAs epitaxial structure', Optics Express, 12(4), pp. 588-592 (23 Feb 2004).
5. R.M De La Rue et al, 'Photonic crystal planar waveguide devices exploiting the thermo-optic effect', Photonic Materials, Devices and Applications**,** Seville, 9th to 11th May 2005, paper 5840-09 (SPIE Procs. 5840)
6. A. S. Jugessur et al, 'Microcavity filters based on hexagonal lattice 2-D photonic crystal structures embedded in ridge waveguides', Photonics and Nanostructures – Fundamentals and Applications, Vol.3, pp. 25 – 29, (August 2005).
7. C. Ciminelli, F. Peluso, V.M.N. Passaro and M.N. Armenise, "Angular Response of Narrow Band 2D-PBG Guided Wave Filters, in 'Microresonators as building Blocks for VLSI Photonics', AIP, Vol. 709 , pp. 439-440, (2004).
8. C. Ciminelli et al, High-Q Guided-Wave Photonic Crystal Extended Microcavity, Post-Deadline papers, pp26-27, European Conference on Optical Communication, ECOC 2004, Stockholm, Sweden, (September 2004).
9. S.M. Weiss et al.' Temperature stability for photonic crystal devices', OPN,'Optics in 2004 special issue', p.35, (Dec 2004).
10. M.W. Geis, S.J. Spector, R.C. Williamson and T.M. Lyszczarz, 'Fast, < 1 Nanosecond, Thermo-Optic Phase Shifters and Switches in SOI', Integrated Photonics Research and Applications (IPRA) Conference, San Diego, paper IMB4, (11-13 April 2005).
11. M.W. Geis, S.J. Spector, R.C. Williamson and T.M. Lyszczarz, 'Submicrosecond, submilliwatt, silicon on insulator thermooptic switch', IEEE Photonics Techn. Lett., **(16)**, pp. 2514-2516, (2004).
12. P. Pottier et al, paper presented at PECS VI meeting, Crete, June 2005.
13. M.Gnan et al, paper presented at ECIO 05 meeting, Grenoble, France, 6th-8th April 2005.
14. M. Gnan et al, paper presented at 13th OWTNM meeting, Grenoble, France, 8th-9th April 2005.